

General probabilistic analysis of simple reinforced slopes using RLEM approach

Pouya Dastpak
Ferdowsi University, Mashhad, Iran
Sobhan Mousavi
Shahid Beheshti University, Tehran, Iran
Reza Jamshidi Chenari
Guilan University, Rasht, Iran
Brigid Cami & Sina Javankhosdel
Rocscience Inc., Toronto, ON, Canada



ABSTRACT

The Random Limit Equilibrium Method (RLEM) is a relatively new method of probabilistic slope stability analysis which uses a combination of 2D random field theory, circular or non-circular limit equilibrium methods and Monte Carlo simulation (or Latin Hypercube simulation). Recent studies have provided probabilistic and deterministic design charts for reinforced slopes with simple geometries. However, the importance of the non-circular Limit Equilibrium Method (LEM) together with optimization techniques to find the critical failure mechanism when considering the influence of spatial variability of soil properties has not previously been addressed. In this paper, similar probabilistic and deterministic design charts for simple reinforced slopes are presented considering both circular and non-circular surfaces, and a spatial correlation length of infinity. RLEM approach is then used to investigate the influence of spatial variability of soil properties on the probability of failure.

RÉSUMÉ

La méthode d'équilibre limite aléatoire (RLEM) est une méthode nouvelle pour l'analyse probabiliste des pentes, qui utilise une combinaison de la théorie des champs aléatoires 2D, de la méthode de glissements circulaires ou non-circulaires, et de simulations Monte Carlo (ou simulations de Latin Hypercube). Des études récentes ont présenté des abaques de calcul probabilistes et déterministes pour des pentes avec des géométries simples, renforcées. Toutefois, l'importance de la méthode d'équilibre limite (LEM) non-circulaire avec des techniques d'optimisation, lorsque l'on considère l'influence de la variabilité spatiale des propriétés du sol n'a pas encore été étudiée. Dans cet article, des abaques de calcul probabilistes et déterministes pour des pentes renforcées simples sont présentés, avec des glissements circulaires et non circulaires, et une longueur de corrélation spatiale de l'infini. L'approche RLEM est ensuite utilisée pour étudier l'influence de la variabilité spatiale des propriétés du sol sur la probabilité de défaillance.

1 INTRODUCTION

Geosynthetic reinforced soil slopes can be designed using modified conventional deterministic limit equilibrium-based methods with circular failure mechanisms (Kitch 1994), log-spiral (Leshchinsky and Boedeker 1989) and two-part wedge (Bathurst and Jones 2001; Jewell 1991). These modifications include the stabilizing contribution of the reinforcement layers that are intersected by potential slip surfaces. While these methods can give quantitative differences in some cases, the differences are typically not large in practical terms. These limit-equilibrium based methods typically provide factors of safety against reinforcement rupture and pullout modes of failure (Javankhosdel and Bathurst 2017). One of the limitations of these methods is the assumption of having prescribed and plausible failure mechanisms. There are different advanced limit equilibrium methods when combined with global and local optimization techniques, help the failure mechanism, first to be non-circular and then to find the weakest failure path (Cami et al. 2018).

An important limitation of deterministic methods for conventional slope stability analyses is that nominal similar slopes may have the same factor of safety but different

probabilities of failure. This is attributed to the random and spatial variability of soil properties. Examples of the quantitative influence of soil property uncertainty on estimates of the probability of failure of unreinforced soil slopes have been demonstrated using conventional limit equilibrium-based methods of slope analysis coupled with Monte Carlo simulation (e.g. Javankhosdel and Bathurst 2014, 2016; Cho 2010; among others). Similar investigations using the random limit equilibrium method (RLEM) have also shown the important influence of soil uncertainty and spatial variability on the probability of failure (e.g. Javankhosdel et al. 2017; Cami et al. 2019). It is reasonable to assume that the uncertainty in soil properties will also influence estimates of the probability of failure for reinforced soil structures.

Kitch (1994) and Kitch et al. (2011) investigated two example reinforced slopes with simple geometry using a circular-slip method of slices approach. The reinforcement arrangement was first determined using design charts by (Schmertmann et al. 1987) that are based on linear and two-part wedge analyses that satisfy only force equilibrium.

Kitch (1994) and Kitch et al. (2011) showed that for a specific uniform length of the reinforcement layers, there is a minimum reinforcement tensile strength to ensure that

the failure mechanism is always external (i.e. the critical failure mechanism passes just beyond the reinforced soil mass). For tensile strength values greater than this minimum value, there is no change in the value of the deterministic factor of safety. They also identified the conditions that lead to internal failure mechanisms where the critical failure geometry is contained wholly within the reinforced soil zone. These internal failures occurred when reinforcement lengths were greater than a critical length for a given reinforcement tensile strength. In such cases, with constant reinforcement length, the factor of safety of the slope varied only with the strength of the reinforcement. They pointed out that for the cases investigated, there is an abrupt change between these two types of failure mechanism where the critical mechanism falls partially within the reinforced soil zone. They then extended the deterministic analyses of the slopes to compute margins of safety in probabilistic terms. They compared the values of the probability of failure for different failure mechanisms and different values of coefficient of variation for the soil friction angle and reinforcement strength and showed that external failure mechanisms give a higher probability of failure compared to internal failure mechanisms.

Javankhoshdel and Bathurst (2017) provided results of deterministic and probabilistic analyses of similar reinforced slopes as Kitch (1994) using Monte Carlo simulation on slopes with a wide range of purely frictional soils ($c = 0, \phi > 0$) and cohesive-frictional soils ($c > 0, \phi > 0$), reinforcement properties, number of reinforcement layers, reinforcement length and slope geometry. Here, c is the soil cohesive strength component and ϕ is the soil friction angle. The link between unreinforced and reinforced slopes with the same factor of safety was also demonstrated. The methods of analysis presented by the (Javankhoshdel and Bathurst 2017) investigation are based on computations that use conventional circular limit equilibrium-based methods for each analysis.

2 PROBLEM DEFINITION AND GENERAL APPROACH

Potential failure mechanisms for simple reinforced soil slopes are illustrated in Figure 1. In the current study, the soil extends below the toe of the slope which permits failure mechanisms to penetrate the foundation. A similar condition was assumed by Javankhoshdel and Bathurst (2017), Kitch (1994) and Kitch et al. (2011). Figure 1c shows a possible composite failure mechanism which in the current study is identified as a transition mechanism between internal and external failure mechanisms.

Figure 2 shows an example slope with $n = 4$ reinforcement layers. A slope height of $H = 5$ m and unit weight, $\gamma = 20$ kN/m³. The slope angle in this study ranged from $\beta = 45^\circ$ to 90° from the horizontal, and the soil friction angle was varied from $\phi = 20^\circ$ to 65° .

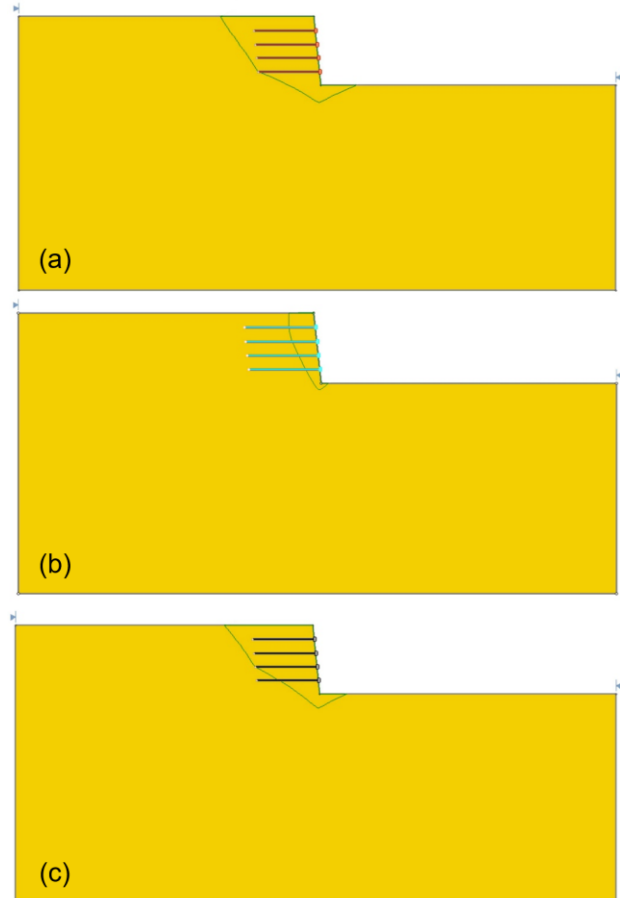


Figure 1. a) External failure mechanism, b) Internal failure mechanism, and c) Transition failure mechanism

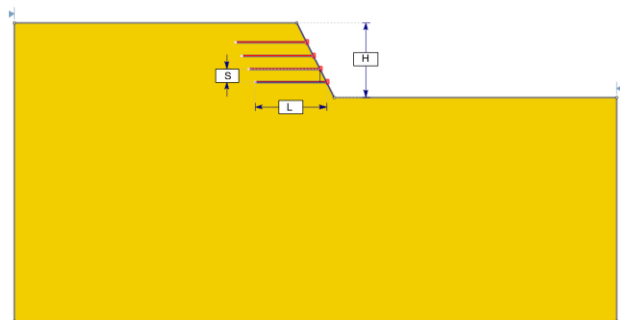


Figure 2. Example slope with: Four layers of geosynthetic reinforcement ($n = 4$) and $H = 5$ m

In the probabilistic analysis presented by Javankhoshdel and Bathurst (2017) the global minimum probability of failure (called fixed method) was used (i.e. the critical failure is first found using a conventional deterministic search and then Monte Carlo simulations are carried out with that slip surface), provided the location of the critical slip surface is known for both failure mechanism cases. They showed that if random variability of the reinforcement tensile strength is not considered (available reinforcement strength is treated deterministically), global

minimum and overall slope (i.e. a different slip surface is found in each Monte Carlo simulation) methods for the case of purely frictional soil slopes give the same results (Javankhosdel and Bathurst 2014).

In this study Slide 2018 software (Rocscience 2018) is used for the analysis of reinforced slopes. To verify the outputs with results presented by Javankhosdel and Bathurst (2017), first circular Bishop's method (for simplicity called circular method hereinafter) is used as the LEM approach and then the GLE method together with a global metaheuristic optimization method (Cuckoo search) and a local optimization technique (Surface Altering Optimization) (for simplicity called non-circular method hereinafter) are used. Monte Carlo simulation is then added to the deterministic analysis to carry out probabilistic analysis in this study. In this study, both global minimum probability of failure (similar to Javankhosdel and Bathurst 2017) and overall slope probability of failure are calculated.

3 DETERMINISTIC SLOPE STABILITY ANALYSIS

3.1 Influence of reinforcement length and tensile strength on failure type

Javankhosdel and Bathurst (2017) and Kitch (1994) showed that for a deterministic analysis, for each value of slope angle and a constant minimum length, F_s is constant for values of reinforcement tensile strength (T) greater than the minimum value to generate only external failure. Here the layer reinforcement strength is denoted as T and is assumed to be the same for all layers. Also, for a constant minimum tensile strength (less than or equal to the threshold tensile strength obtained for external failure), F_s is constant for the values of reinforcement length greater than the minimum value to generate only internal failure mechanisms. Therefore, for each slope case, they showed that it is possible to generate a single contour plot of factors of safety for external and internal failure mechanisms. However, the minimum values of reinforcement tensile strength and reinforcement length are in general different for external and internal failure mechanisms.

Figures 3 and 4 show the combinations of minimum values of reinforcement length and minimum tensile strength to generate only external failure mechanisms (Solid lines). In other words, all other combinations of reinforcement length and strength falling above solid lines for each slope angle case will result in external failure mechanisms only. In these figures, dashed lines are plots showing combinations of reinforcement length and tensile strength below which only internal failure mechanisms will occur. Figure 3 is a comparison between the results of the Slide 2018 software and results presented by Javankhosdel and Bathurst (2017). Figures 4a, 4b and 4c show the results of the comparison between the non-circular method and circular method and for different slope angles of 45°, 63° and 84°, respectively.

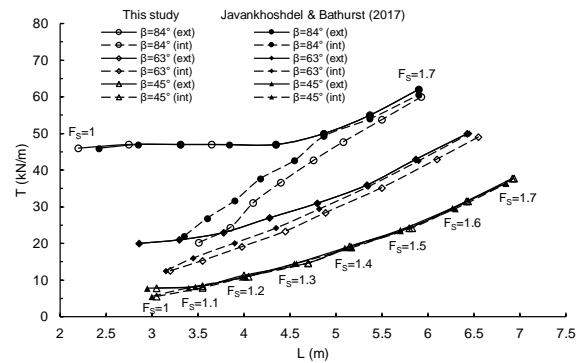


Figure 3. Threshold values of reinforcement length (L) and tensile strength (T) to generate only internal failure mechanisms and only external failure mechanisms ($H = 5$ m, $n = 4$, $\gamma = 20$ kN/m³, $\phi = 30^\circ$, $c = 0$)

Figure 3 shows that the circular method results in this paper are in good agreement with those presented by Javankhosdel and Bathurst (2017). This figure shows that there is a transition between these two types of behaviours which becomes more pronounced with increasing slope angle. For a slope with $\beta = 45^\circ$ and all other conditions the same (i.e. $H = 5$ m, $n = 4$, $\gamma = 20$ kN/m³, $\phi = 30^\circ$, $c = 0$), the two plots are essentially the same and thus describe a unique locus of reinforcement length and strength that neatly divide slope failure mechanisms into external and internal types. Also shown in this figure are the corresponding factors of safety (F_s). The same string of factor of safety values applies to all plots in this figure. For each plot, the factor of safety to generate each data point increases with increasing L and T .

Figures 4a, 4b and 4c show the difference between the results of non-circular and circular methods to get the same F_s values. It can be seen in this figure that, to get the same factor of safety using the circular and non-circular methods, for external failure mechanism, the non-circular method requires larger tensile strength with longer reinforcement layers. On the other hand, to get the same value of F_s with internal failure mechanism, the non-circular method requires larger tensile strength with shorter reinforcement layers. The difference between the results of non-circular and circular is significant. Also, it can be seen in this figure that, the transition zone between the results of the non-circular method is much larger than the results of the circular method for larger values of slope angle (e.g. $\beta = 84^\circ$)

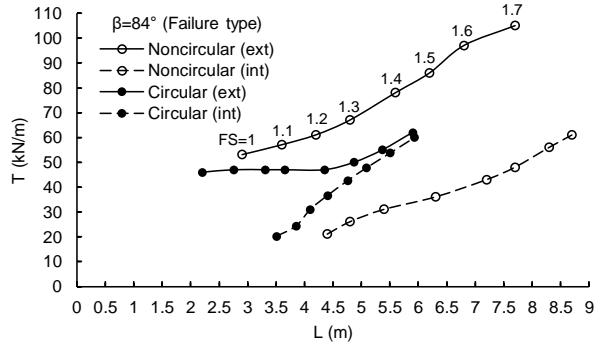
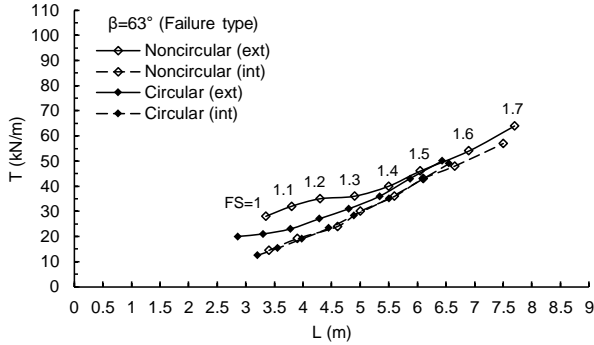
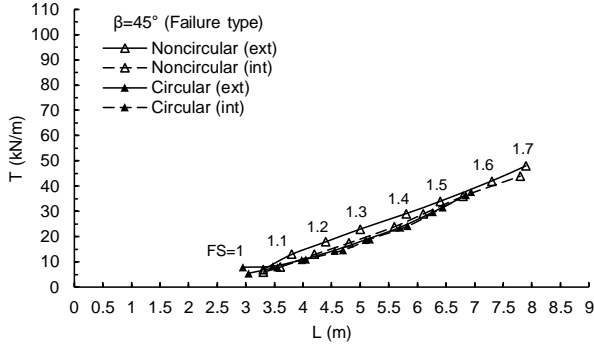


Figure 4. Threshold values of reinforcement length (L) and tensile strength (T) to generate only internal failure mechanisms and only external failure mechanisms ($H = 5$ m, $n = 4$, $\gamma = 20$ kN/m³, $\phi = 30^\circ$, $c = 0$) and for a) $\beta = 45^\circ$ b) $\beta = 63^\circ$ c) $\beta = 84^\circ$

Figure 5 shows contour plots for the factor of safety for the same example slope in Figure 4c with $\beta = 84^\circ$ and using the non-circular method. The upper region corresponds to external failure mechanisms and the lower region corresponds to internal failure mechanisms. The locus of points dividing the two regions in Figure 5 matches the same curve for $\beta = 84^\circ$ in Figure 4c for $F_s \geq 1.1$. As it is mentioned before, the transition zone between the internal and external failure mechanisms is very large using the non-circular method.

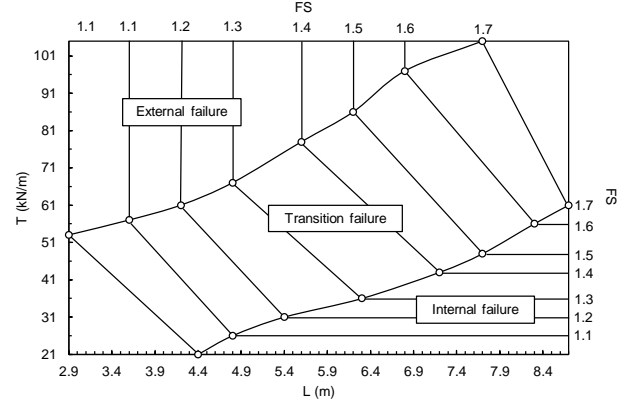


Figure 5. Contour plots for F_s values corresponding to internal, transition and external failure mechanisms for $\beta = 84^\circ$, $H = 5$ m, $n = 4$, $\gamma = 20$ kN/m³, $\phi = 30^\circ$ and $c = 0$

4 PROBABILISTIC SLOPE STABILITY ANALYSIS

4.1 General

Stationary estimates of the coefficient of variation of friction angle and unit weight of soil reported in the literature are $COV_\phi = 0.2$ and $COV_\gamma = 0.1$, respectively (e.g. Phoon and Kulhawy 1999) which are used in this study.

Similar to Javankhoshdel and Bathurst (2017), 5000 Monte Carlo simulations were shown to be sufficient to compute P_f in the probabilistic analysis.

4.2 Probabilistic analysis results for purely frictional soil slopes ($c = 0$, $\phi > 0$)

4.2.1 External failure cases

To create probabilistic slopes stability charts for external failure mechanism in this study, the first step was to find the critical combination of reinforcement length and tensile strength to just generate a (deterministic) external failure for a target factor of safety. Example combinations of L and T for a particular slope case to just generate an external failure for a range of prescribed factors of safety are the loci of joint internal and external failure L and T data in Figures 3 and 4 using circular and non-circular methods, respectively. Next, for each critical mechanism (circular or non-circular failure) corresponding to these conditions two probabilistic analyses using the global and overall slope methods are carried out.

Javankhoshdel and Bathurst (2017) showed that using the circular method with the global minimum probability of failure, changing the slope angle, reinforcement tensile strength, reinforcement length and the number of reinforcement layers does not change the maximum probability of failure. For the same (deterministic) value of F_s corresponding to the critical external failure mechanism, P_f is the same. This is because the location of the critical slip surface passes just beyond the reinforced zone, and hence the values of F_s and P_f depend only on the factored soil strength. Based on these observations they presented

a single chart with plots of maximum probability of external failure versus factor of safety for different factored soil friction angles using the circular method with global minimum probability of failure as shown in Figure 6. Superimposed on this chart are the results of probabilistic analysis of this study with the global minimum method and the circular approach. It can be seen in this figure that the results are in a good agreement.

Here, ϕ_f is the factored soil friction angle computed as:

$$\phi_f = \tan^{-1} \left(\frac{\tan \phi}{F_s} \right) \quad [1]$$

It can be seen in Figure 6 that for the same mean value of F_s , slopes with higher values of ϕ_f have a greater maximum probability of failure. This is because slopes with stronger soil (higher ϕ_f) can generate an external failure with lower tensile strength reinforcement layers and shorter length. As the factored soil friction angle becomes greater the critical external failure mechanisms become shallower (Javankhoshdel and Bathurst 2017).

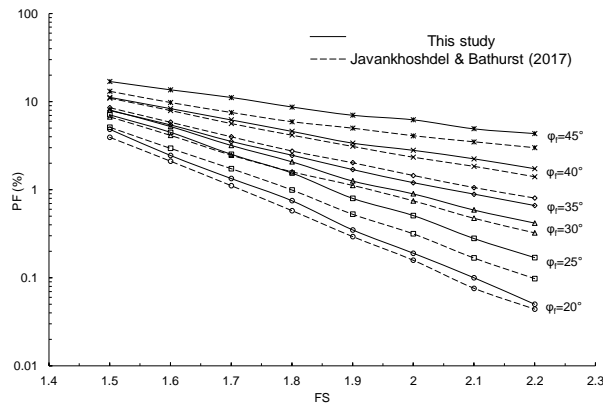
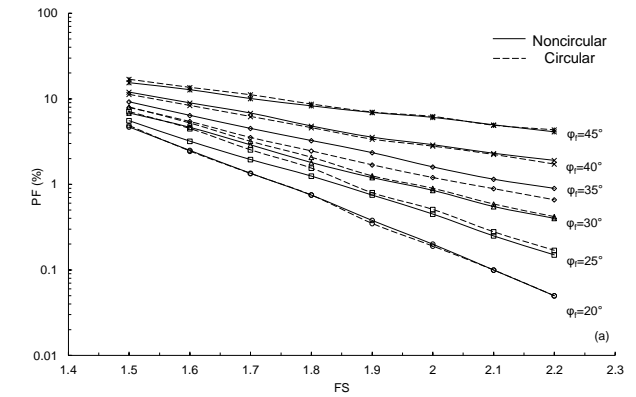


Figure 6. Maximum probability of external failure (P_f) for reinforced soil slopes with factored friction angle (ϕ_f) versus mean factor of safety in the range $1.5 \leq F_s \leq 2.2$

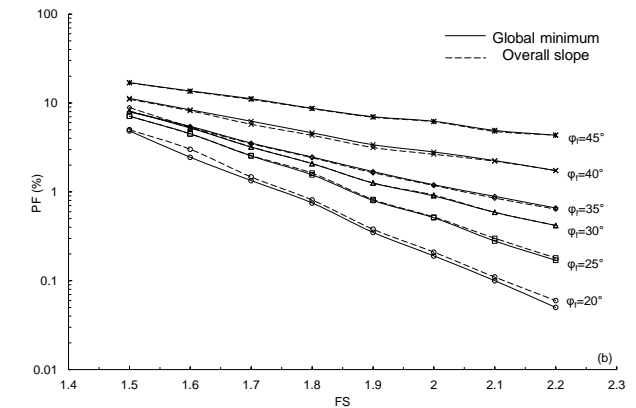
Figures 7a, 7b, and 7c show the comparison between the non-circular and circular methods, global minimum versus overall slope methods for circular and non-circular approaches, respectively for external failure mechanism. It can be seen in these figures that, for external failure mechanism, the probability of failure does not change by changing the search method to find the critical failure mechanism. In other words, as it was shown in Figure 4, to get the same F_s using the non-circular method as the F_s using the circular method, larger tensile strengths and longer reinforcement layers should be considered; however, with the same F_s using both methods the same global minimum and overall slope probability of failure will be achieved.

4.2.2 Internal failure cases

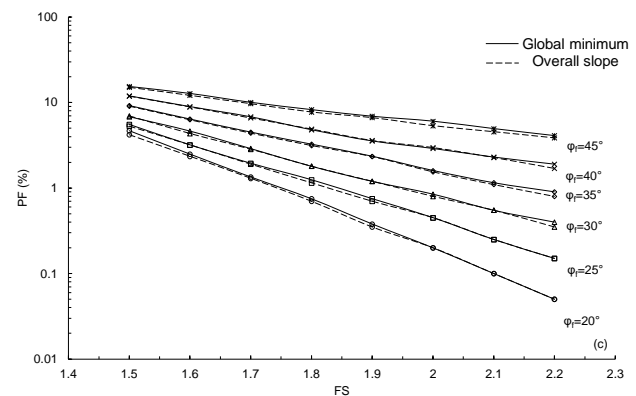
To change the failure mechanism from external failure to internal failure, longer reinforcement layers must be used if other parameters are kept the same (e.g. see Figure 3 and 4).



a)



b)



c)

Figure 7. Maximum probability of external failure (P_f) for reinforced soil slopes with factored friction angle (ϕ_f) versus mean factor of safety in the range with $1.5 \leq F_s \leq 2.2$ for a) non-circular vs circular method b) global minimum versus overall slope method for circular method c) global minimum versus overall slope method for non-circular method

Javankhoshdel and Bathurst (2017) presented the same charts as Figure 6 for internal failure mechanism and for the maximum probability of internal failure using the circular method and the global minimum Pf. Figure 8 presents such a chart for $\beta = 45^\circ$, different values of ϕ_f and $1.5 \leq F_s \leq 2.2$. Superimposed on this chart are the results of the current study using the circular method with global minimum probability of failure. It can be seen that the results of both studies are in a good agreement.

To generate data for this chart for a target value of F_s , critical combinations of T and L values that generate internal failure only were found first. Then, probabilistic analyses using the global minimum method were carried out to calculate the maximum (upper-bound) probability of failure for the corresponding deterministic factor of safety (F_s). Figure 8 shows that for the same value of F_s , plots with higher ϕ_f values have a higher maximum probability of failure. The reason is that the probability of internal failure depends largely on the value of the tensile strength of the reinforcement. For slopes with stronger soil (higher ϕ_f), the required tensile strength of the reinforcement layers to achieve the same F_s value is lower; therefore, increasing ϕ_f increases P_f .

It should be noted that higher probabilities of failure may be acceptable in the case of internal failure of reinforced soil slopes based on similarities to other high strength-redundant soil structure systems. Thus, the 1% probability of failure criterion is shown as the upper line in Figure 8.

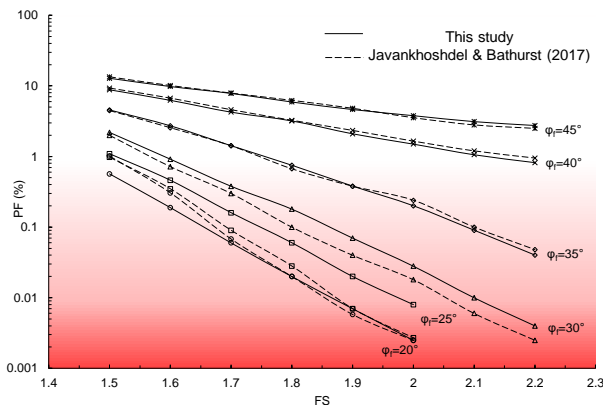


Figure 8. Maximum probability of internal failure for reinforced soil slopes with different values of factored friction angle ϕ_f versus mean factor of safety in the range $1.5 \leq F_s \leq 2.2$ for slopes with $\beta = 45^\circ$.

Figures 9a, 9b, and 9c show the comparison between the non-circular and circular methods, global minimum versus overall slope methods for non-circular and circular approaches, respectively for internal failure mechanism. It can be seen in Figure 9a that, changing the search for the failure mechanism from circular to non-circular method does not change the probability of failure for a global probability of failure and for the same F_s . In other words, as it was shown in Figure 4, to get the same F_s using the non-circular method as the F_s using the circular method larger

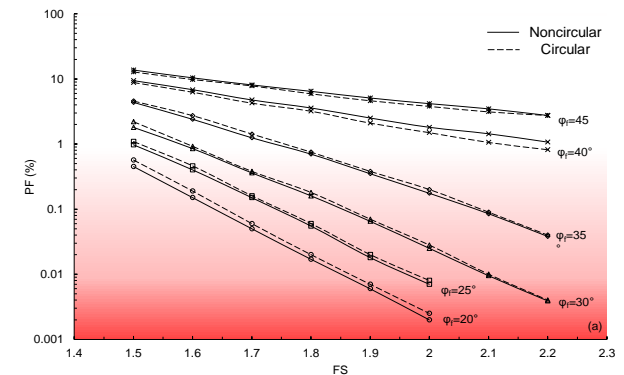
tensile strength and shorter reinforcement layers should be considered; however, with the same F_s using both methods the same global minimum probability of failure will be achieved.

On the other hand, Figures 9b and 9c show that, unlike Figures 7b and 7c, for the same value of F_s , changing the search method of probability of failure from global minimum to overall slope, reduces the probability of failure dramatically, i.e. global minimum probability of failure is conservative for design purposes compared to the overall slope probability of failure and the difference becomes larger between the two methods by reducing ϕ_f and P_f (i.e. when the slope is safer)

4.3 Probabilistic analysis results for purely frictional soil slopes considering spatial variability ($c = 0, \phi > 0$)

4.3.1 Non-Circular RLEM

The non-circular RLEM used in this study is a combination of the non-circular method (non-circular GLE method, metaheuristic global optimization method (Cuckoo search) and the Surface Altering local optimization technique) and the random field generated using the Local Average Subdivision Method (LAS) proposed by Fenton and Vanmarcke (1990). Studies showed that, in many cases, for the same number of surfaces, a larger number of slip surface with lower factors of safety were detected using Cuckoo search method and Surface Altering Optimization technique compared to the number determined from conventional grid or slope search techniques (Cami et al. 8). When used in conjunction with a non-circular search these optimization methods can be very effective at locating slip surfaces with lower safety factors. Although the option is referred to as "optimization," it can also be considered an additional search method.



a)

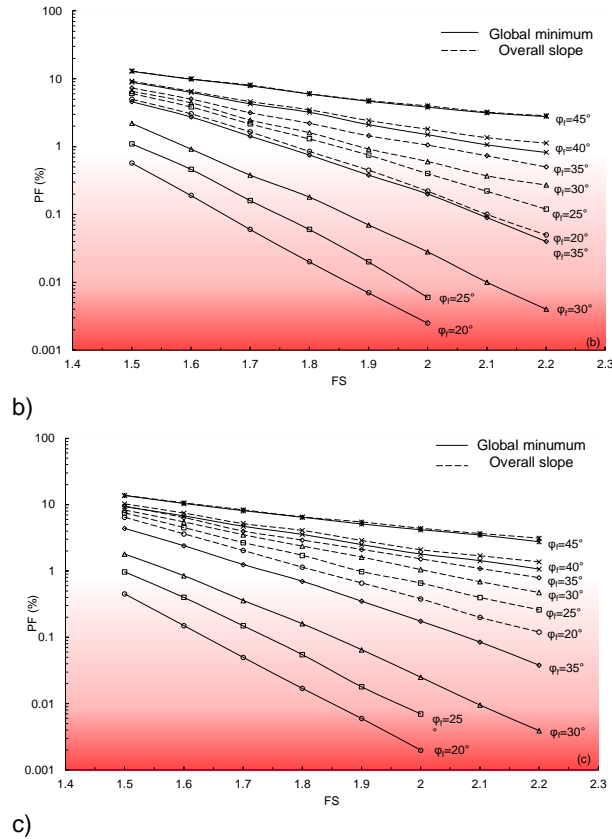


Figure 9. Maximum probability of internal failure for reinforced soil slopes with different values of factored friction angle ϕ_f versus mean factor of safety in the range $1.5 \leq F_s \leq 2.2$ for slopes with $\beta = 45^\circ$ for a) non-circular vs circular method b) global minimum versus overall slope method for circular method c) global minimum versus overall slope method for non-circular method.

The combination of Cuckoo search with optimization and random fields generated using LAS method helps to locate the critical slip surface in the spatially variable field. The circular RLEM was presented for the first time by Javankhosdel et al. (2017). However, the disadvantage of the circular RLEM, as mentioned by them is that the circular RLEM cannot capture irregular shapes of failure. This is especially noticeable in cases with highly fluctuating random fields. However, the optimization technique in the non-circular RLEM, moves the vertices along the slip surface to find the lowest factor of safety. Moving the vertices allows cells with lower values of soil strength in the random field mesh to be found and therefore weaker (more critical) failure paths are located.

4.3.2 RLEM results

The maximum probability of failure in Figures 7c and 9c for external and internal failure mechanism, respectively, and for non-circular overall slope failure mechanism are for the case with $\phi_f = 45^\circ$. For this case (and for the case with $F_s = 1.5$) different spatial correlation length is considered.

Luo and Bathurst (2018) provided different numbers for the vertical spatial correlation length starting from 0.625 which is equal to the compaction length of reinforced retaining wall. In this study, six different values of 0.625, 2, 5, 10, 20, 100 for vertical spatial correlation length are considered for both internal and external failure mechanisms and for $\phi_f = 45^\circ$. The results are presented in Figure 10. It can be seen in Figure 10 that internal failure mechanism gives smaller probability of failure compared to the external failure mechanism for the same spatial correlation length which is expected. The interesting observation in this figure is, in both cases, as the spatial correlation length increases, there is a worst-case spatial variability for the spatial correlation length of about 10m which is equal to two times the height of the slope, i.e. probability of failure increases up to this point and then there is a sudden decrease in the probability of failure. Thus, the results of probabilistic analysis ignoring spatial variability of soil properties are no longer upper bound for design purposes.

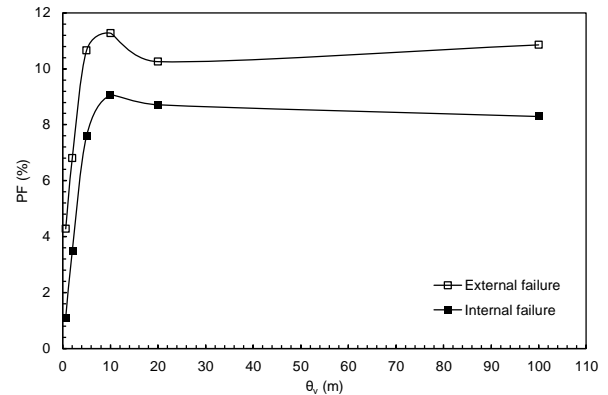


Figure 10. Probability of failure for external and internal failure mechanisms calculated using non-circular method and for different values of $\theta_v = 0.645m, 2, 5, 10, 20$ and $100m$ and $\theta_h = 500m$ ($\phi_f = 45^\circ$ and $F_s = 1.5$)

5 CONCLUSIONS

This study reports the results of the probabilistic slope stability analysis of reinforced slopes using Monte Carlo simulation together with circular and non-circular Limit Equilibrium Methods. Two main mechanisms of failure of geosynthetic reinforced slopes were investigated: 1) external failure mechanisms that comprise critical slip surfaces that pass beyond the reinforced zone, and 2) internal mechanisms where critical slip surfaces intersect all the reinforcement layers.

In this study, the probabilistic results of non-circular and circular methods are compared for internal and external failure mechanism. The results of global minimum and overall slope probability of failure are also compared for both failure mechanisms.

It can be seen for the external and internal failure mechanisms that, changing the shape of the failure mechanism from circular to non-circular does not change the probability of failure significantly. Also, for external failure mechanism, overall slope and global minimum

probabilities of failure are the in agreement for the same factor of safety. However, overall slope probability of failure is much smaller for the internal failure mechanism compared to the global minimum probability of failure.

To investigate the influence of spatial variability of soil properties on the probability of failure of reinforced slopes for external and internal failure mechanisms, Random Limit Equilibrium Method (RLEM) analysis was used. In the RLEM analysis, a large constant horizontal spatial correlation length and different values of vertical spatial correlation length were used. It is shown that the internal failure mechanism gives lower probability of failure compared to the external failure mechanism. Also, for the cases presented in this study there is a maximum probability of failure for the values of correlation length equal to twice the height of slopes, i.e. the cases that ignore the spatial variability of soil properties are not conservative for design purposes.

6 REFERENCES

- Bathurst, R.J. and Jones, C.J.F.P. 2001. Chapter 17: Earth retaining structures and reinforced slopes. Geotechnical and Geoenvironmental Engineering Handbook, Kluwer Academic Publishing, Norwell, MA, U.S.A. (R.K. Rowe, Editor): 1088.
- Cami B., Javankhoshdel S., Yacoub T., Bathurst R.J. 2018. 2D Spatial Variability Analysis of Sugar Creek Embankment: Comparative Study. In: Shehata H., Desai C. (eds) Advances in Numerical Methods in Geotechnical Engineering. GeoMEast 2018. Sustainable Civil Infrastructures. Springer, Cham.
- Cho, S.E. 2010. Probabilistic assessment of slope stability that considers the spatial variability of soil properties. ASCE Journal of Geotechnical and Geoenvironmental Engineering, 136(7): 975–984.
- Fenton, G.A. and Vanmarcke, E.H., 1990. Simulation of random fields via local average subdivision. *Journal of Engineering Mechanics*, 116(8), pp.1733-1749.
- Javankhoshdel, S. and Bathurst, R.J. 2014. Simplified probabilistic slope stability design charts for cohesive and $c-\phi$ soils. Canadian Geotechnical Journal, 51(9): 1033-1045.
- Javankhoshdel, S. and Bathurst, R.J. 2016. Influence of cross-correlation between soil parameters on probability of failure of simple cohesive and $c-\phi$ slopes. Canadian Geotechnical Journal, 53 (5): 839-853.
- Javankhoshdel, S. and Bathurst, R. J. 2017. Deterministic and probabilistic failure analysis of simple geosynthetic reinforced soil slopes. Geosynthetics International, 24, No. 1, 14–29.
- Javankhoshdel, S., Luo, N., and Bathurst, R. J. 2017. Probabilistic analysis of simple slopes with cohesive soil strength using RLEM and RFEM. *Georisk: Assessment and Management of Risk for Engineered Systems and Geohazards*, 11(3), 231-246.
- Jewell, R.A. 1991. Application of revised design charts for steep reinforced slopes. *Geotextiles and Geomembranes*, 10(3): 203-233.
- Kitch, W. 1994. Deterministic and probabilistic analyses of reinforced soil slopes, Ph.D. Dissertation, University of Texas, Austin TX.
- Kitch, W.A., Gilbert, R.B. and Wright, S.G. 2011. Probabilistic assessment of commercial design guides for steep reinforced slopes: Implications for design. Reston, VA: ASCE Proceedings of Georisk 2011, Atlanta, Georgia, d 20110000.
- Leshchinsky, D. and Boedeker, R.H. 1989. Geosynthetic reinforced soil structures. *Journal of Geotechnical Engineering*, 115(10): 1459-1478.
- Luo, N, and Bathurst, R.J. 2018. Probabilistic analysis of reinforced slopes using RFEM and considering spatial variability of frictional soil properties due to compaction. *Georisk: Assessment and Management of Risk for Engineered Systems and Geohazards*, 12:2, 87-108.
- Phoon, K.K. and Kulhawy, F.H. 1999. Characterization of geotechnical variability. *Canadian Geotechnical Journal*, 36(4): 612-624.
- RocScience Inc. 2018. Slide Version 2018 – 2D Limit Equilibrium Slope Stability Analysis. www.rocscience.com, Toronto, Ontario, Canada.
- Schmertmann, G., Chouery-Curtis, V., Johnson, R. and Bonaparte, R. 1987. Design charts for geogrid-reinforced soil slopes. In proceedings of Geosynthetics '87. Industrial Fabrics Association International, Roseville, MN: 108-120.